JOURNAL OF ENERGY, MATERIALS, AND INSTRUMENTATION TECHNOLOGY

Journal Webpage https://jemit.fmipa.unila.ac.id/

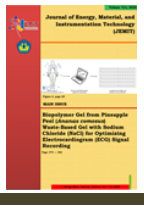

Mechanical Homogenization of Biochar Porous Structures Using Two-Dimensional RVE: A Study of Finite Element Methods on the Relationship of Actual Porosity and Effective Elastic Modulus

Naufal Nabiha Luthfiantoro, and Ahmad Atif Fikri

Mechanical Engineering, University of Malang, Malang, Indonesia

Article Information

Article history:
Received January 23, 2026
Received in revised form January 30, 2026
Accepted February 28, 2026

Keywords: *Mechanical Properties; Porosity; Finite Element Method; Homogenization; Microstructure*

Abstract

This study analyzes the mechanical response of porous biochar using a 2D FEM–RVE homogenization approach to investigate the effect of mesh-based actual porosity and microstructural arrangement on stiffness and stress concentration. Three types of RVEs (regular, shifted, and random) were simulated at several porosity levels for five biochar types (wood, bamboo, grass, RHB, and sludge) under the assumption of linear elastic material. Loading was applied using kinematic uniform boundary conditions (KUBC), and the effective elastic modulus (E_{eff}) was extracted from the homogenization response, while the maximum stress (σ_{max}) was recorded as an indicator of stress localization. Results show that E_{eff} decreases nonlinearly with increasing ϕ_{mesh}, and at the same porosity, more continuous microstructures retain higher stiffness. Normalization into relative modulus (E_rel) reveals overlapping trends across biochar types for the same RVE, allowing the influence of solid-phase properties to be separated from pore shape effects. These findings underscore the importance of using actual porosity and simultaneously evaluating global stiffness and local stress indicators in interpreting the mechanics of porous biochar.

Informasi Artikel

Proses artikel:
Diterima 3 Januari 2026
Diterima dan direvisi dari 30 Januari 2026
Accepted 28 Februari 2026

Kata kunci: *Mechanical Properties; Porosity; Finite Element Method; Homogenization; Microstructure*

Abstrak

Penelitian ini menganalisis respons mekanik biochar berpori menggunakan pendekatan homogenisasi FEM–RVE dua dimensi untuk mengkaji pengaruh porositas aktual berbasis mesh dan susunan mikrostruktur terhadap kekakuan dan konsentrasi tegangan. Tiga tipe RVE (teratur, tergeser, dan acak) disimulasikan pada beberapa tingkat porositas untuk lima jenis biochar (wood, bamboo, grass, RHB, dan sludge) dengan asumsi material elastik linier. Pembebanan diterapkan menggunakan kinematic uniform boundary condition (KUBC), kemudian modulus elastis efektif (EE_{eff}) diekstraksi dari respons homogenisasi dan tegangan maksimum (σ_max) dicatat sebagai indikator lokalisasi tegangan. Hasil menunjukkan E_{eff} menurun nonlinier seiring meningkatnya ϕ_{mesh}, dan pada porositas yang sama mikrostruktur yang lebih kontinu mempertahankan kekakuan lebih tinggi. Normalisasi menjadi modulus relatif (E_rel) memperlihatkan kecenderungan kurva yang saling berimpit lintas biochar pada RVE yang sama, sehingga pengaruh sifat fase padat dapat dipisahkan dari pengaruh bentuk pori. Temuan ini menegaskan pentingnya penggunaan porositas aktual dan evaluasi simultan kekakuan global serta indikator tegangan lokal dalam interpretasi mekanika biochar berpori..

1. Introduction

Biochar is a porous carbon material produced through the process of pyrolysis biomass under oxygen-limited conditions (M. Zhang dkk., 2022). In recent years, biochar has been widely studied for its potential in a wide range

* Corresponding author.
E-mail address: naufal.nabiha.2205146@stundents.um.ac.id

of engineering and environmental applications, including soil amelioration, environmental remediation, adsorbent materials, as well as as a supporting component in sustainable construction and materials systems. The main characteristic of biochar lies in its complex and multiscale pore structure, which results in a high specific surface area and superior physical–chemical function. These characteristics make biochar an interesting functional material to be developed further.

In general, the mechanical properties of porous materials are determined by a combination of the properties of the solid phase of their constituent and the shape of the pore microstructure (Long dkk., 2021; Xu, 2023). Increased porosity generally leads to a decrease in effective elastic modulus due to a reduction in the load-supporting solid phase fraction and the appearance of a stress concentration around the pores. This kind of porosity-rigidity relationship has been widely studied in various engineered porous material systems, such as lattice structures and Triply Periodic Minimal Surface (TPMS) (Long dkk., 2021; Xu, 2023), and is widely accepted as a basic framework in the mechanical analysis of porous materials.

However, the application of these porosity–mechanical properties relationships to biochar becomes more complex because its microstructures are irregular, heterogeneous, and often disconnected (Zhang et al., 2025; Z. Zhang et al., 2023). At high porosity levels, the mechanical load tends to be concentrated on the remaining solid phase path, thereby increasing the potential for localized deformation and a significant decrease in rigidity. This condition suggests that the mechanical description of biochar cannot always be adequately represented through global porosity parameters alone.

The Finite Element Method (FEM) numerical approach has been widely used to bridge the relationship between microstructures and the mechanical response of porous materials (Huang dkk., 2024; Xu, 2023). In the study of porous materials in general, the global mechanical response is known to be influenced by the multiscale interaction between the microstructure and the solid-phase properties of its constituents, as also reported in a variety of heterogeneous porous media systems (Lv et al., 2023). However, most existing studies still use design target porosity assumptions or simple homogenization parameters, so they do not fully represent the actual geometry of the microstructure analyzed numerically. In addition, studies that systematically evaluate the effect of the microstructure of the Representative Volume Element (RVE) on the elastic response of biochar and explicitly separate the contribution of the solid-phase stiffness properties of biochar from the influence of pore shape in a single consistent homogenization framework are still very limited. As a result, mechanistic understanding of the role of the actual porosity of discretized mesh results and the arrangement of microstructures in controlling the elastic response of porous biochar has not been fully quantified in the literature (Huang et al., 2024; Long et al., 2021; Z. Wang et al., 2024; Xu, 2023; Z. Zhang et al., 2023).

Therefore, this study analyzes the mechanical homogenization of porous biochar using a two-dimensional FEM–RVE approach with variations in microstructure and porosity levels. The analysis focused on the relationship between the actual porosity obtained from the mesh geometry and the effective elastic modulus. Normalization of elastic modulus into relative modulus is applied to separate the influence of the solid-phase stiffness properties of biochar from the influence of pore shape. Through this framework, the research aims to provide a mechanistic understanding of the role of porosity and the microstructure of microstructures in controlling the elastic response of porous biochar (Huang et al., 2024; Long et al., 2021; Z. Wang et al., 2024; Xu, 2023; Z. Zhang et al., 2023).

2. Methodology

2.1 General Framework of FEM–RVE Homogenization

Mechanical analysis of porous biochar was performed using a numerical homogenization based approach *Representative Volume Element* (RVE) with the element method up to (*Finite Element Method*, FEM). The main goal of this approach is to extract the effective elastic properties of the macro scale from the mechanical responses of porous microstructures that are explicitly resolved at the micro scale (Huang et al., 2024; Z. Wang et al., 2024). In the framework of first-order homogenization, the macro strain field is represented through the boundary conditions on the RVE domain, while the local voltage and strain fields are calculated numerically and averaged to obtain effective properties. The FEM–RVE approach has been widely used in heterogeneous porous materials due to its ability to capture the influence of microstructure arrangements, solid phase connectivity, as well as deformation localization potential that cannot be represented by simple analytical homogenization models (Krzaczek et al., 2022; Menke et al., 2021). In the context of porous materials, global mechanical responses are often controlled by the presence of a minimum solid load path and the distribution of local stress in small-sectional ligaments, so explicit analysis at the microscale is crucial.

2.2 RVE Microstructure Design

The biochar microstructure is represented using a two-dimensional RVE that models a solid–void two-phase system. Three types of microstructures were used to separate the effect of the regularity and heterogeneity of solid load paths on mechanical responses, namely RVE1 (regular), RVE2 (displaced with intermediate heterogeneity), and RVE3 (random/irregular). All RVEs have the same domain size and the same number of pore features equalized at each porosity level, so the difference in mechanical response mainly reflects the difference in the topology and connectivity of the solid phase (Krzaczek et al., 2022; Menke et al., 2021).

The RVE1 is built as a periodic void array with a continuous solid load path. The increase in porosity is done by uniformly enlarging the size of the void while maintaining geometric periodicity. RVE2 was developed from RVE1 by applying controlled shifting to the void position, so that the symmetry and continuity of the load path is reduced without changing the pore size statistics. RVE3 is formed through random placement of voids with rules *non-overlap*, which results in a more fragmented and heterogeneous solid-phase network. For RVE3, multiple realizations were used at each porosity condition to capture the statistical variability of the mechanical response (Huang et al., 2024; Z. Wang et al., 2024).

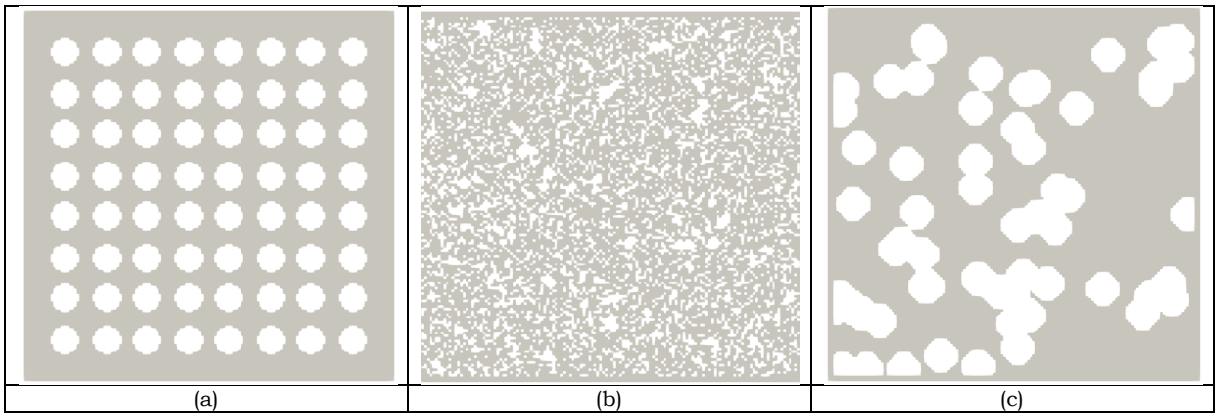

Figure 1. Examples of porous biochar two-dimensional RVE geometry: (a) RVE1 is regular (Bataillou dkk., 2022), (b) RVE2 shifted (Chakma & Luo, 2024) and (c) random RVE3. The three microstructures are equalized in domain size and pore base statistics(Pingaro dkk., 2019)

2.3 Definition of Actual Porosity

The porosity used in the analysis is defined as the actual porosity of the discretized mesh result, which is denoted as . In solid–void two-dimensional systems, porosity is calculated as the ratio of the area of the void phase to the total area of the domain,ϕ_{mesh}

$$\phi_{\text{mesh}} = \frac{A_{\text{void}}}{A_{\text{total}}}$$

The mesh-based porosity definition was chosen because the mechanical response is calculated directly on the discrete geometry used in the FEM simulation. Thus, the actual porosity value expressed as φ_mesh represents the conditions of the structure that are actually numerically analyzed. Some studies have shown that nominal porosity or design target porosity can differ from actual porosity due to geometric discretization and mesh manufacturing processes, especially in porous structures with minimally sized ligaments. Therefore, the use of φ_mesh ensures consistency between the structural descriptors used in the analysis and the simulated numerical domains (Thompson et al., 2021; Zhuang et al., 2022).

2.4 Biochar Solid Phase Material

The solid phase of biochar is modeled as an isotropic linear elastic material. The material parameters used are the Young's modulus of solid phase and Poisson ratio. The five types of biochar are differentiated by value, while they are kept constant for all cases to separate the influence of the material scale from the influence of the microstructure of the microstructure $E_s \nu E_s \nu$(Behazin dkk., 2016). This approach is in line with the practice of modeling porous materials and cellular structures, where effective mechanical properties are seen as the result of the interaction between the material properties of the strut and relative density. (Krzaczek et al., 2022; Menke et al., 2021).

Table 1. The elastic parameters of the solid phase of biochar used in the FEM simulation

Code	Jenis biochar	Young's Modulus of Solid Phase, (GPa)E_s	Rasio Poisson, (-)ν	References
B1	Wood / softwood chip	10.0	0.25	**[11]**
B2	Grass / wheat-straw	5.0	0.25	**[11]**
B3	Bamboo	7.0	0.25	**[12] [13]**
B4	RHB (rice husk biochar)	8.0	0.25	**[12] [13]**
B5	Sludge	4.0	0.25	**[12] [13]**

It should be noted that the solid-phase Young modulus values for wood-based biochar (10 GPa) and grass-based biochar (5 GPa) are adopted directly from the results of nanomechanical measurements reported by E_s(Behazin dkk., 2016). The study showed that the biochar from pyrolysis of lignocellulose biomass has intrinsic stiffness on the order of a few gigapascals, with significant differences depending on the type of feedstock.

Meanwhile, for bamboo-based biochar, rice husk biochar (RHB), and sludge, until this writing stage, no reference has been found that states the exact same value as the value used in the simulation. Therefore, the three materials are treated as assumption parameters that are still within the stiffness range of pyrolysis carbon materials as reported in nanoindentation studies and mechanical analysis of biochar and biochar-based biocomposites E_s(Das dkk., 2016; Zickler et al., 2006). This approach can be accounted for as long as it is explicitly stated as an assumption and is used in the context of FEM-based parametric studies to evaluate the relative influence of solid-phase properties on the effective mechanical response of porous structures.

2.5 Homogenization Boundary Conditions

Mechanical homogenization is carried out using *a displacement-based Kinematic Uniform Boundary Condition* (KUBC). In this scheme, the displacement field at the RVE boundary is forced following the linear macro strain field,

$$u_i(\mathbf{x}) = \varepsilon_{ij}^{\text{macro}}\, x_j$$

For uniaxial loading in the direction, displacement is applied to the left and right boundaries of the domain so as to produce the target macro strain. One additional reference point is locked to eliminate the motion of rigid objects. KUBC was chosen because it is numerically stable and theoretically provides an estimate of the upper limit of the elastic properties effective over other boundary conditions $x\varepsilon_{xx}$(Krzaczek et al., 2022; Menke et al., 2021).

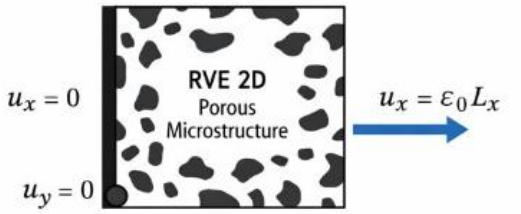

Figure 2. Scheme of application of KUBC on two-dimensional RVE for elastic homogenization.

2.6 FEM Settlement and Effective Quantity Extraction

The linear elastic boundary problem in the RVE domain is solved using *finite element solver* SfePy. The domain is discretized into two-dimensional triangular elements, and the elastic equilibrium equation is solved using *linear solver* directly. Once the displacement field is obtained, the strain and voltage fields are calculated at the level of the solid-phase element (Krzaczek et al., 2022; Menke et al., 2021).

The mean macro voltage in the direction of loading is defined as the average area of the voltage component in the solid phase,

$$\bar{\sigma}_{xx} = \frac{1}{A_s}\int_{\Omega_s} \sigma_{xx}\,(\mathbf{x})\,\mathrm{d}A$$

The effective elastic modulus is then calculated from the ratio between the average stress and the applied macro strain,E_{eff}

$$E_{\text{eff}} = \frac{\bar{\sigma}_{xx}}{\varepsilon_{xx}^{\text{macro}}}$$

In addition to the homogeneous response, the maximum voltage of σ_{max} is recorded as an indicator of local stress concentration related to the heterogeneity of the microstructure and the presence of critical ligaments (Saunier et al., 2024; Tian et al., 2022).

2.7 Normalization and Relative Modulus

In order to separate the influence of the solid phase property from the influence of the pore microstructure, the elastic modulus is effectively normalized into a relative modulus. Normalization is carried out by dividing the solid phase Young modulus of each biochar,$E_{rel}E_{eff}$

$$E_{\text{rel}} = \frac{E_{\text{eff}}}{E_s}$$

This approach allows an evaluation of the internal consistency of homogenization results and emphasizes the role of the shape and arrangement of pore microstructures separately from the properties of solid-phase materials. In linear elastic regimes, the modulus curve relative to the same porosity is expected to show a tendency to constrict each other for various materials, indicating that the elastic response is primarily controlled by the geometry and interconnectedness of the structure. Behavior E_{rel}*collapse* This kind has been widely reported in studies of lattice structures and engineered porous materials (Judawisastra et al., 2025; Lv et al., 2023; M. Zhang et al., 2022).

2.8 Simulation and Data Processing Pipeline

All simulations were run systematically for a combination of RVE type, biochar type, and porosity level. Each case is assigned a unique identity and all input–output parameters are recorded in a structured table format to guarantee repeatability and traceability of results. Quality checks were performed at the pre-simulation (solid-phase connectivity, mesh quality) and post-simulation (reasonableness of values and) stages to minimize numerical artifacts that could affect the interpretation of the results $E_{\text{eff}}\sigma_{\max}$(Krzaczek et al., 2022; Zhuang et al., 2022).

3. Results and Discussions

3.1 Results

Internal Validation of Elastic Models

Before discussing the relationship between porosity and mechanical response, internal validation was performed to ensure that the entire simulation was still in a linear elastic state and was not affected by numerical errors. This validation is carried out by examining the linearity of the relationship between the macro stress and strain, as well as the stability of the elastic modulus value effective against small variations of applied strain (Krzaczek et al., 2022; Menke et al., 2021). All simulations show a linear stress–strain relationship over the strain range used, so that the mechanical response obtained can be considered representative of the elastic behavior of the material.

In addition, based on the examination of the local strain field as commonly reported in the FEM analysis of porous materials (Z. Zhang dkk., 2023), the highest strain concentration was identified in solid-phase ligaments with a minimum cross-section. Meanwhile, most domains exhibit a relatively homogeneous strain distribution, a characteristic typical of elastic responses in multiscale porous materials (Menke et al., 2021). This distribution pattern is also in line with previous findings on engineered porous structures, which suggest that strain localization is primarily controlled by critical ligament geometry and not by numerical instability (Behazin dkk., 2016), so it can be concluded that the simulation is in a linear elastic condition with no indication of local plasticity.

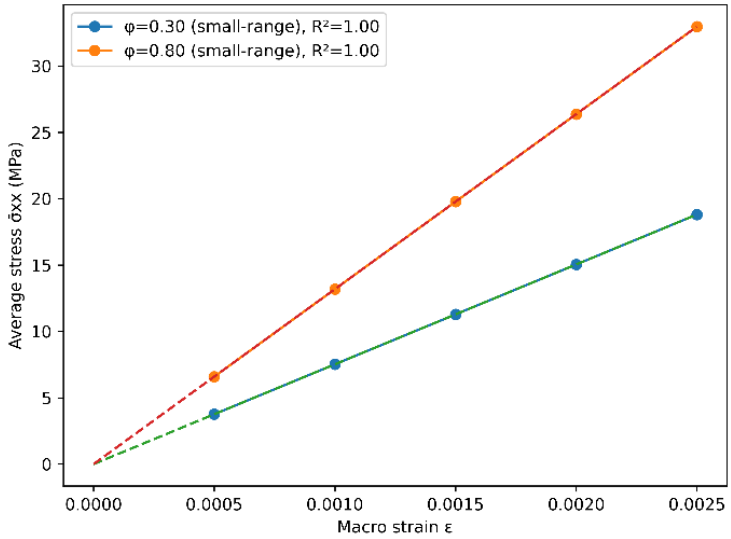

Figure 3. An example of a macro stress–strain relationship resulting from FEM–RVE homogenization showing a linear elastic response.

Figure 3 shows the relationship between the mean macro stress and the applied macro strain for one representative case (RVE1–Wood,). The resulting curve shows a very clear linear relationship over the entire analyzed strain range, with no indication of nonlinearity or deviation from the linear elastic behavior.$\bar{\sigma}_{xx}\varepsilon_{xx}^{macro}\phi_{mesh} \approx 0.30$

This linearity confirms that the mechanical response of RVE is entirely within the range of linear elastic behavior, so that the assumption of isotropic elastic material applied in the FEM simulation remains valid and consistent with the homogenization theory (Krzaczek dkk., 2022).

This figure shows verification that the simulation is in a linear elastic condition because for the two contrasting porosity conditions, and , the relationship between the mean stress and the macro strain remains a straight line at the small strain range used (up to) with for both so that no nonlinear deviation is found at the modulus extraction working range, while the difference in line slope between the two porosities shows that the change in porosity changes the load path and the degree of tension localization in the remaining solid ligaments.$\phi_{mesh} = 0.30\phi_{mesh} = 0.80\bar{\sigma}_{xx}\varepsilon\varepsilon = 0.0025R^2 = 1.00$

Effect of Porosity on Effective Elastic Modulus

Figure 4 shows the variation of the elastic modulus effective against the actual porosity for all RVE types and biochar types. In general, an increase in porosity leads to a decrease that is nonlinear in nature. This behavior reflects a decrease in the fraction of the solid phase that serves as a load-bearer, as well as an increase in the concentration of tension in the remaining ligaments as porosity increases, as reported in studies of porous materials and heterogeneous structures$E_{\text{eff}}\phi_{\text{mesh}}E_{\text{eff}}$(Palomar & Barluenga, 2022; Zickler dkk., 2006). However, at high porosity, the decrease in rigidity becomes more pronounced because—as described in the study of engineered porous structures (Zhang et al., 2025; M. Zhang et al., 2022)The disconnection of the solid load path leads to the dominance of the small-cross-sectional critical ligaments that control the overall mechanical response.

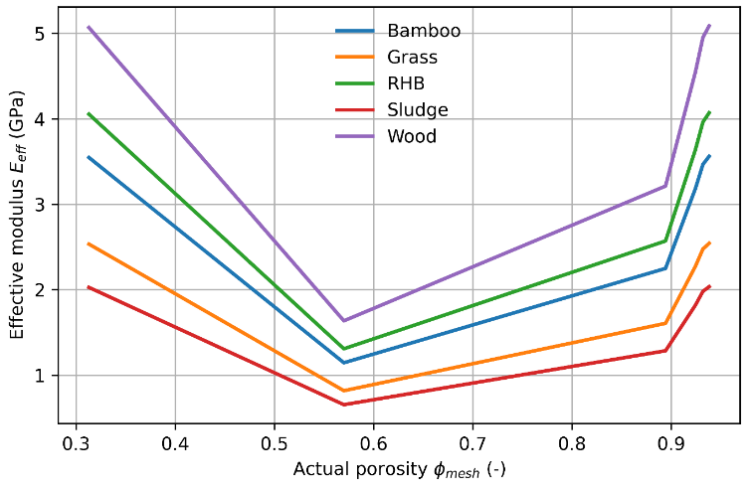

Figure 4. The elastic modulus relationship is effective against the actual porosity for different types of RVE.$\mathbf{E_{eff}\phi_{mesh}}$

A sharp downward bend on the curve against occurs because when the actual porosity increases, the solid-phase network loses load path continuity nonlilaterally, the connective ligaments thin and part of the effective load path disappears, so that the global stiffness drops rapidly over a given porosity range $\boldsymbol{E_{eff}\phi_{mesh}}$(De Carolis dkk., 2024) Meanwhile, the visible increase in high porosity can occur when the configuration/placement of the pore makes the residual load path more efficient in the direction of load so that some structures retain relatively higher rigidity even when the porosity is large, not because the material changes to nonlinear $\boldsymbol{E_{eff}}$(Biswas & Ma, 2022) And this graph is important because it confirms that porosity alone is not always sufficient as the sole foundation of rigidity, geometry and pore space configuration are decisive so that the curve – necessary to map the stiffness sensitivity effectively – while associating the shape of the curve with the shape of the microstructure observed through stress localization $\boldsymbol{E_{eff}\phi_{mesh}}$

Role of RVE Microstructure Arrangement

Comparisons between RVE types show that the arrangement of microstructures has a significant influence on values at the same porosity level. RVE1, which has a more regular void arrangement, produces the highest value because the solid phase path still forms a relatively straight and continuous load trajectory. In contrast, RVE3 with random pore distribution showed the lowest values, which were related to the fragmentation of solid-phase tissues and an increased tendency to localize tension in the minimum cross-sectional ligaments. This behavior is in line with findings in heterogeneous porous materials, where the regularity of the microstructure arrangement plays an important role in maintaining the continuity of load transfer and the stability of the elastic mechanical response $\boldsymbol{E}_{\text{eff}}\boldsymbol{E}_{\text{eff}}\boldsymbol{E}_{\text{eff}}$(Thompson dkk., 2021).

RVE2 displays a response that is somewhere between the two extremes, reflecting the intermediate level of microstructural heterogeneity. These findings indicate that, as reported in studies of heterogeneous porous materials (Behazin dkk., 2016), in addition to total porosity, the topology and connectivity of the solid phase play a dominant role in controlling the effective rigidity of porous materials, especially when the solid-phase network begins to lose continuity (Thompson dkk., 2021).

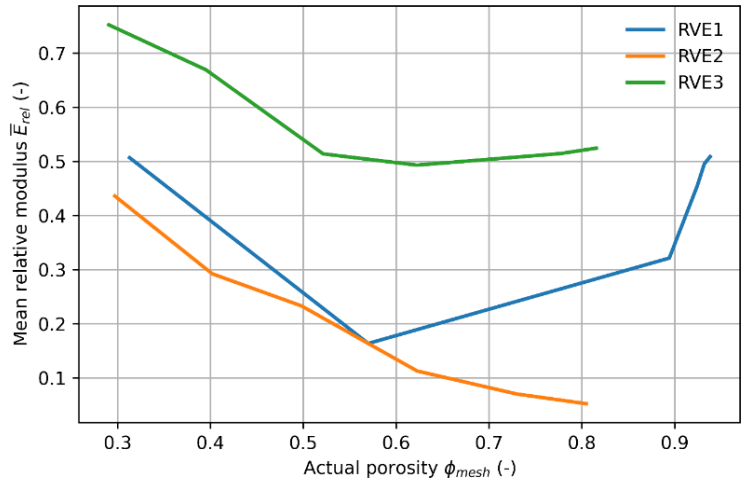

Figure 5. Comparison between RVE types at the same porosity level.$\mathbf{E_{eff}}$

Figure 5 Average relative modulus comparison to actual porosity for RVE1–RVE3. The difference in curves between RVEs at the same porosity shows that the microstructural arrangement (solid-phase load path connectivity and continuity) contributes significantly to effective stiffness, regardless of variations in solid-phase stiffness scales.$\bar{E}_{rel}\phi_{mesh}$

Curve shape – in RVE1 it differs from RVE2 and RVE3 in that the more regular/periodic RVE1 maintains a more continuous solid-phase load path so that the decrease in relative rigidity tends to be more controlled, whereas the shifted RVE2 disrupts symmetry and accelerates the weakening of the ligament connectivity so that it descends more sharply, while the random RVE3 results in a network of load paths that are affected by irregularity/percolation so that the response can be more pronounced $\bar{E}_{rel}\phi_{mesh}\bar{E}_{rel}$*Robust* at a certain porosity range but more sensitive to local configurations that are aligned with the intrinsically non-periodic pore character of biochar (Somboon dkk., 2025), so from this data RVE1 is not automatically more ideal than RVE2/RVE3 because the ideal depends on the purpose: RVE1 is more ideal as a stable and easily reproducible baseline/benchmark for controlled studies, while RVE3 is more statistically representative to generalize the response of random porous materials in an RVE-based homogenization framework (Pingaro dkk., 2019)

Relative Modulus and Separation of Material Influences Microstructure

In order to evaluate the role of the microstructure arrangement of the microstructure independently of the properties of the solid phase, the elastic modulus is effectively normalized to a relative modulus. Figure 6 shows the relationship to all types of biochar in each type of RVE.$E_{rel}E_{rel}\phi_{mesh}$

In the same type of RVE, the curves of different types of biochar tend to overlap, especially in RVE with a more regular arrangement of microstructures. This phenomenon shows that, as reported in studies of lattice structures and engineered porous materials E_{rel}(Zickler dkk., 2006), the absolute value difference is mainly controlled by the mechanical properties of the solid phase of biochar. In contrast, the shape of the relationship between modulus and porosity is more determined by the arrangement and connectivity of the microstructure, which regulates how the load is transferred through the solid-phase network E_{eff}(Palomar & Barluenga, 2022). Behavior *curve collapse* This kind is generally understood as an indicator of the internal consistency of the homogenization process and has been widely used as a conceptual validation in the analysis of elastic porous materials (Lee & al., 2024).

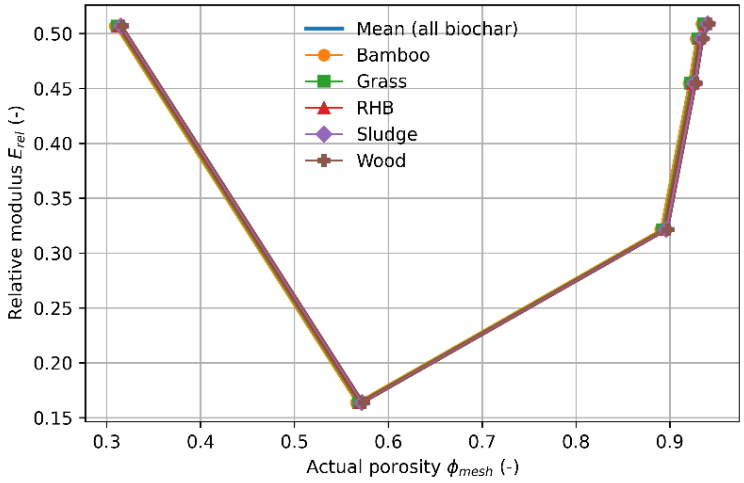

Figure 6. The modulus relationship relative to the actual porosity for different types of biochar in a single type of RVE.$\mathbf{E_{rel}}$

Voltage Distribution and Deformation Localization

The von Mises stress distribution in the RVE domain shows that the maximum stress concentration is mainly localized in the solid-phase ligaments that connect adjacent pores. This localization pattern is in line with the character of heterogeneous elastic porous materials, where the minimum cross-sectional ligament acts as a critical point of load transfer and tends to experience the highest stress concentrations (Thompson dkk., 2021).

The intensity and location of the voltage concentration are greatly influenced by the microstructure arrangement and the level of porosity. In RVE with a regular arrangement, the voltage distribution is relatively symmetrical and more even along the main load path(Guo et al., 2023). In contrast, in RVEs with random pore distribution, the voltage field becomes highly heterogeneous with sharp stress peaks localized to specific ligaments, as also reported in heterogeneous porous structure studies (Palomar & Barluenga, 2022). The maximum stress value increases as porosity increases, which indicates increased susceptibility to local fault initiation, although the global mechanical response still shows linear elastic behavior $\boldsymbol{\sigma}_{\mathbf{max}}$(Behazin dkk., 2016).

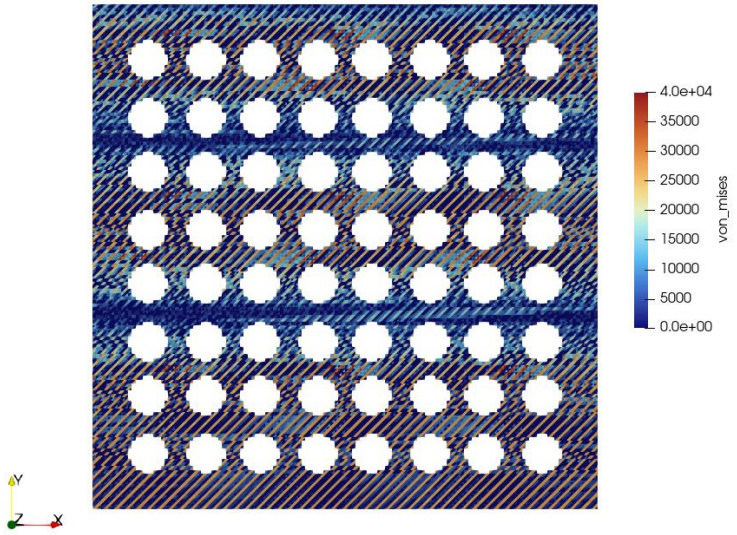

Figure 7. Example of the von Mises voltage distribution on RVE

Summary of Quantitative Results

A summary of the actual porosity values, effective elastic modulus, relative modulus, and maximum stress for the entire combination of RVE type and biochar type are presented in Table 3.1. This table provides a comprehensive quantitative overview of the influence of porosity and the microstructure arrangement of microstructures on the mechanical response of porous biochar.$\boldsymbol{\phi_{mesh} E_{eff} E_{rel} \sigma_{max}}$

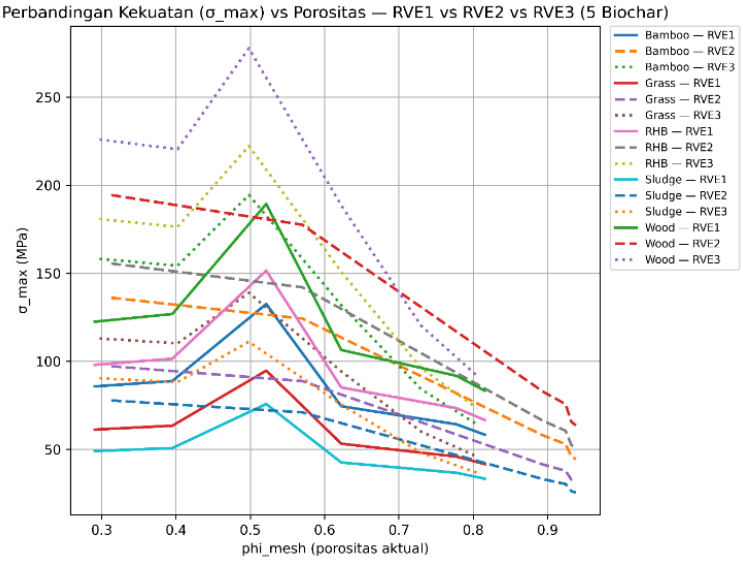

Figure 8. Summary of the mechanical parameters of FEM–RVE homogenization results for all combinations of RVE and biochar types.

The figure shows the relationship between the local maximum voltage () and the actual porosity () for five types of biochar in the three RVE configurations. In general, the entire curve exhibits a nonlinear response to porosity, where it increases and reaches peak values at low–medium porosity (), then decreases at higher porosity. This pattern reflects an increased stress concentration when the solid-phase path is continuous but limited, while the decrease in high porosity is related to weakened solid-phase connectivity and reduced ability of porous structures to transfer stress effectively, as reported in studies of heterogeneous elastic porous materials [11], [14]. $\boldsymbol{\sigma_{max}\phi_{mesh}\sigma_{max}\phi_{mesh} \approx 0,3–0,5\sigma_{max}}$The difference in values at the same porosity confirms the role of the microstructure of RVE and the solid-phase properties of biochar on local stress distribution [18]. Wood and bamboo-based biochar tend to show higher than thatching, rice husk, and mud-based biochar,$\boldsymbol{\sigma_{max}\sigma_{max}}$ The wood and bamboo biochar on the graph are affected because the more "skeletonized" lignocellulose feedstock is able to maintain a hierarchical architecture and a high carbon fraction so that its micromechanical properties (hardness/indentation response) can reach high values when the original structure is maintained (Q. Wang dkk., 2025), while straw and rice husk biochar tend to carry larger ash/mineral fractions (including inorganic components that modify the pyrolysis pathway and increase the heterogeneity of solids) so that the load-bearing carbon frame becomes more disrupted and effectively lowers the solid

rigidity seen by homogenization (Puri et al., 2024), and in mud-based biochar this difference is usually stronger because the character of sludge-derived biochar is generally rich in minerals/inorganic components and more complex/heterogeneous so that it is mechanically less ideal as an elastic load-bearing framework than lignocellulose biochar (Zhou et al., 2024), so that when in the simulation the differences between biochars are modeled through solid phase parameters, the output directly follows the solid stiffness scale and is physically consistent with the carbon-ash microstructure differences reported in the recent literature indicating a stiffer load path but more susceptible to voltage localization. In the context of this study, it is used as an indicator of elastic microstructural vulnerability, so that the results obtained represent a comparison of the relative mechanical response between RVE and between biochar types, not as a measure of material collapse strength.$\boldsymbol{E_0 E_{eff} \sigma_{\max}}$

3.2 Discussions

This discussion focuses on how the actual mesh-based porosity (φ_mesh), variation in the RVE microstructure arrangement, and the overall solid phase nature of biochar impact the elastic response expressed through effective elastic modulus (E_eff), relative modulus (E_rel), and maximum stress (σ_max). The focus is not only on showing trends, but explaining the mechanisms that cause those trends to appear in porous materials.

Increased φ_mesh consistently lowers E_eff across all RVE types and all biochar. Physically, as the pores increase, the dense part of the load carrier decreases and the load transfer path becomes narrower or more severed, so that the effective rigidity also decreases. This pattern is common in porous materials and cellular structures, as reported in TPMS/lattice structures and engineered porous systems (Zhang et al., 2025; M. Zhang et al., 2022) and in porous carbon materials with interconnected dense-pore tissues (Gibson & Ashby, 1982; Sadek & al., 2024). The use of φ_mesh also reinforces the consistency of interpretation because FEM responses are calculated on discrete geometry that is actually simulated; The target/design porosity may deviate from the actual porosity due to discretization and mesh fabrication, especially when minimum ligaments are the determining factor (Thompson et al., 2021; Zhuang et al., 2022).

At the same φ_mesh value, the difference in the microstructure of the RVE still results in a noticeable E_eff difference. RVEs with more connected solid-phase networks tend to maintain higher E_eff, while more random/fragmented microstructures are more prone to localized deformation so that E_eff descend (Huang et al., 2024; Z. Zhang et al., 2023). These findings are in line with studies of foam/porous materials that emphasize that not only the number of pores, but also the distribution of pore size and the connectivity of solid tissues play a major role in determining the effective elastic modulus (Gibson & Ashby, 1982; Li dkk., 2021). Normalization of E_eff into E_rel helps to separate the influence of solid-phase stiffness scale from the influence of pore shape: in the same type of RVE, inter-biochar E_rel curves that tend to overlap each other show that E_eff differences are mainly due to solid-phase modulus differences, while the pattern of decline in porosity is more determined by the arrangement of microstructures; This approach is commonly used as an internal consistency check in the study of porous structures/lattices (Stuart et al., 2025), and is also reported on porous carbon systems (Gibson & Ashby, 1982). At very high porosity, small inter-curve deviations are still possible due to the increasingly sensitive response to minimum ligament details and local irregularities (Behazin et al., 2016; Z. Zhang et al., 2023)

In terms of local response, increased porosity is generally followed by increased σ_max, which indicates that stress tends to accumulate in the remaining ligaments as the solid phase fraction decreases; This phenomenon is a common feature of porous materials and is usually sharper in microstructures with low affinity (Behazin et al., 2016; Z. Zhang et al., 2023). In complex structured carbon materials, the heterogeneity of solid tissues also often gives rise to stress concentration points that are relevant to initial mechanical susceptibility (Gibson & Ashby, 1982; Sadek & al., 2024). In addition, multiscale studies on biochar systems in composite matrices show that microstructural inconsistencies can trigger dominant local responses even though the discussion is still at low load (Manna & al., 2025). Therefore, σ_max in this study is best treated as an indicator of elastic microstructural vulnerability, not a measure of material collapse strength.

4. Conclusions

The results showed that mesh-based actual porosity (φ_{mesh}) was the most consistent parameter in explaining stiffness attenuation, where E_{eff} systematically decreased as φ_{mesh} increased for all combinations of RVE type and biochar type. Although φ_{mesh} the same, the microstructure of RVE still produces a noticeable E_{eff} difference; RVEs with more connected solid-phase networks maintain higher E_{eff}, while more fragmented microstructures decrease E_{eff} due to localization of deformation. The relative modulus (E_{rel}) pattern indicates that absolute E_{eff} variation is more influenced by the rigidity of the solid phase, while the decrease in porosity is determined by the microstructure. In addition, the local maximum stress (σ_{max}) increases with φ_{mesh} and appears on critical ligaments, confirming that this indicator is more relevant to the vulnerability of elastic microstructures than to the collapse strength of the material. This study presents a controlled and reproductive 2D FEM–RVE framework, confirms the role of φ_{mesh} as a numerical structure descriptor, and presents E_{eff}–E_{rel}–σ_{max} metrics to assess the stiffness and vulnerability of microstructures simultaneously.

However, this research model has limitations because it is still 2D, so the three-dimensional effects, spatial anisotropy, and 3D connectivity are not fully represented, and the solid phase is assumed to be isotropic linear elastic without considering plasticity, damage, or cracking. For follow-up research, it is recommended to develop a 3D RVE to evaluate network anisotropy and connectivity, incorporate a nonlinear model or damage to attribute σ_{max} to failure initiation, and add numerical robustness studies related to RVE size, random realization variations, and mesh sensitivity to establish limits on applicability and uncertainty of outcomes.

Acknowledgement

This research was completed well thanks to the support and assistance from various parties. The author would like to thank all who have provided guidance, input, and motivation during the research process.

5. Bibliography

Bataillou, G., Lee, C., Monnier, V., Gerges, T., Sabac, A., Vollaire, C., & Haddour, N. (2022). Cedar Wood-Based Biochar: Properties, Characterization, and Applications as Anodes in Microbial Fuel Cell. *Applied Biochemistry and Biotechnology*, *194*(9), 4169–4186. https://doi.org/10.1007/s12010-022-03997-3

Behazin, E., Ogunsona, E., Rodriguez-Uribe, A., Mohanty, A. K., Misra, M., & Anyia, A. O. (2016). Mechanical, chemical, and physical properties of wood and perennial grass biochars for possible composite application. *BioResources*, *11*(1), 1334–1348.

Biswas, P., & Ma, J. (2022). Spatial pore distribution: An approach to uncouple the strength–porosity trade-offs. *Journal of Materials Science*, *57*(1), 411–421. https://doi.org/10.1007/s10853-021-06587-6

Chakma, P., & Luo, Y. (2024). Impact of Regular and Irregular Pore Distributions on the Elasticity of Porous Materials: A Microstructure-Free Finite Element Study. *Materials*, *17*(18), 4490. https://doi.org/10.3390/ma17184490

Das, O., Sarmah, A. K., & Bhattacharyya, D. (2016). Nanoindentation assisted analysis of biochar added biocomposites. *Compos. Part B Eng.*, *91*, 219–227.

De Carolis, S., Putignano, C., Soria, L., & Carbone, G. (2024). Effect of porosity and pore size distribution on elastic modulus of foams. *International Journal of Mechanical Sciences*, *261*, 108661. https://doi.org/10.1016/j.ijmecsci.2023.108661

Gibson, L. J., & Ashby, M. F. (1982). The mechanics of three-dimensional cellular materials. *Proc. R. Soc. A*, *382*(1782), 43–59. https://doi.org/10.1098/rspa.1982.0088

Guo, W., Wang, F., Wu, Y., Jiang, J., & Xu, W. (2023). New insights into freezing behavior of saturated and air-entrained porous media via a micromechanics-based thermo-hydro-mechanical model. *Water Resour. Res.*, *59*(4). https://doi.org/10.1029/2022WR034211

Huang, W., Meng, F., Liu, J., & Wong, T. (2024). Development of compaction localization in Leitha limestone: Finite element modeling based on synchrotron X-ray imaging. *J. Geophys. Res. Solid Earth*, *129*(8). https://doi.org/10.1029/2024JB028868

Judawisastra, N., Wicaksono, S., Dwianto, Y., Mahyuddin, A., Dirgantara, T., & Zuhal, L. (2025). Comprehensive prediction of the relative modulus of strut-based gyroid lattice structures employing an ML-based surrogate model. *J. Biomed. Mater. Res. B Appl. Biomater.*, *113*(8). https://doi.org/10.1002/jbm.b.35613

Krzaczek, M., Nitka, M., & Tejchman, J. (2022). A novel DEM-based pore-scale thermo-hydro-mechanical model for fractured non-saturated porous materials. *Acta Geotech.*, *18*(5), 2487–2512. https://doi.org/10.1007/s11440-022-01746-8

Lee, J., & al., et. (2024). Engineering a hierarchy of disorder: A new route to synthesize high-performance 3D nanoporous all-carbon materials. *Adv. Mater.*, *36*(32). https://doi.org/10.1002/adma.202402628

Li, S., Xu, J., Liu, Z., & Zhang, Y. (2021). A 3D RVE-based computational homogenization approach for predicting the effective elastic properties of periodic porous materials. *Comput. Mater. Sci.*, *199*, 110738. https://doi.org/10.1016/j.commatsci.2021.110738

Long, K., Chen, Z., Zhang, C., Yang, X., & Saeed, N. (2021). An aggregation-free local volume fraction formulation for topological design of porous structures. *Materials*, *14*(19), 5726. https://doi.org/10.3390/ma14195726

Lv, W., Hu, J., Liu, J., Xiong, C., & Zhu, F. (2023). Porosity effect on the mechanical properties of nano-silver solder. *Nanotechnology*, *34*(16), 165701. https://doi.org/10.1088/1361-6528/acb4f3

Manna, K., & al., et. (2025). Microstructural characterization of ball-milled biochar and its reinforcing efficiency in biobased thermoplastic polyurethane. *ACS Sustain. Resour. Manage.*, *2*(9), 1719–1730. https://doi.org/10.1021/acssusresmgt.5c00225

Menke, H., Maes, J., & Geiger, S. (2021). Upscaling the porosity–permeability relationship of a microporous carbonate for Darcy-scale flow with machine learning. *Sci. Rep.*, *11*(1). https://doi.org/10.1038/s41598-021-82029-2

Palomar, I., & Barluenga, G. (2022). Acoustic assessment of multiscale porous lime–cement mortars. *Materials*, *16*(1), 322. https://doi.org/10.3390/ma16010322

Pingaro, M., Reccia, E., & Trovalusci, P. (2019). Homogenization of Random Porous Materials With Low-Order Virtual Elements. *ASCE-ASME Journal of Risk and Uncertainty in Engineering Systems Part B: Mechanical Engineering*, *5*(3), 030905. https://doi.org/10.1115/1.4043475

Puri, L., Hu, Y., & Naterer, G. (2024). Critical review of the role of ash content and composition in biomass pyrolysis. *Frontiers in Fuels*, *2*, 1378361. https://doi.org/10.3389/ffuel.2024.1378361

Sadek, H., & al., et. (2024). Well-ordered bicontinuous nanohybrids from a bottom-up approach for enhanced strength and toughness. *Nano Lett.*, *24*(35), 11020–11027. https://doi.org/10.1021/acs.nanolett.4c03157

Saunier, J., Chinnayya, A., Kaeshammer, É., Reynaud, M., & Genetier, M. (2024). Mesoscale modeling of the shock-to-detonation transition of pressed HMX. *Propellants Explos. Pyrotech.*, *49*(9). https://doi.org/10.1002/prep.202400125

Somboon, S., Schlichenmaier, S., Thumanu, K., Pakawanit, P., Yodda, S., Sukitprapanon, T.-S., & Lawongsa, P. (2025). Transformations in physicochemical properties and pore structure of biochar derived from rice straw revealed by synchrotron techniques. *Scientific Reports*, *15*(1), 23641. https://doi.org/10.1038/s41598-025-08772-y

Thompson, E., Tomenchok, K., Olson, T., & Ellis, B. (2021). Reducing user bias in X-ray computed tomography-derived rock parameters through image filtering. *Transp. Porous Media*, *140*(2), 493–509. https://doi.org/10.1007/s11242-021-01690-3

Tian, Y., Zhan, W., Jamal, A., & Dini, D. (2022). On the microstructurally driven heterogeneous response of brain white matter to drug infusion pressure. *Biomech. Model. Mechanobiol.*, *21*(4), 1299–1316. https://doi.org/10.1007/s10237-022-01592-3

Wang, Q., Ji, Y., Sridharan, M. M., Lang, L., Zou, Y., Kirk, D. W., & Jia, C. Q. (2025). Unlocking extreme anisotropy in monolithic biochar hardness. *Biochar X*, *1*(1), 0–0. https://doi.org/10.48130/bchax-0025-0007

Wang, Z., Ding, X., Liu, J., & Fu, L. (2024). Numerical simulations on compression behaviors of laminated shale based on digital image technology and the discrete element method. *Sci. Rep.*, *14*(1). https://doi.org/10.1038/s41598-024-66333-1

Xu, X. (2023). Grain-level numerical simulations for the effective elasticity of weakly cemented sandstones. *ACS Omega*, *8*(37), 33610–33621. https://doi.org/10.1021/acsomega.3c03802

Zhang, M., Xu, M., Li, J., Shi, W., & Chen, Y. (2022). Compressive behavior of hollow triply periodic minimal surface cellular structures manufactured by selective laser melting. *Rapid Prototyping Journal*, *29*(3), 569–581. https://doi.org/10.1108/RPJ-04-2022-0128

Zhang, Z., Qi, Y., Wei, B., Bao, H., & Xu, Y. (2023). Application strategy of finite element analysis in artificial knee arthroplasty. *Front. Bioeng. Biotechnol.*, *11*. https://doi.org/10.3389/fbioe.2023.1127289

Zhou, Y., Gao, J., Yang, X., Ni, H., Qi, J., Zhu, Z., Yang, Y., Fang, D., Zhou, L., & Li, J. (2024). Recent Progress in Sludge-Derived Biochar and Its Role in Wastewater Purification. *Sustainability*, *16*(12), 5012. https://doi.org/10.3390/su16125012

Zhuang, Ł., Shin, H., Yeom, S., Pham, C., & Kim, Y. (2022). A novel method for estimating subresolution porosity from CT images and its application to homogeneity evaluation of porous media. *Sci. Rep.*, *12*(1). https://doi.org/10.1038/s41598-022-20086-x

Zickler, G. A., Schöberl, T., & Paris, O. (2006). Mechanical properties of pyrolysed wood: A nanoindentation study. *Philos. Mag.*, *86*, 1373–1386.